THE JOURNAL OF PHYSICAL CHEMISTRY C

ARTICLE

pubs.acs.org/JPCC

Theoretical Studies of Transition-Metal-Doped Single-Walled Carbon Nanotubes

Ya Kun Chen,[†] Lei Vincent Liu,[†] Wei Quan Tian,[‡] and Yan Alexander Wang*[,†]

[†]Department of Chemistry, University of British Columbia, 2036 Main Mall, Vancouver, BC V6T 1Z1, Canada

[‡]State Key Lab of Urban Water Resource and Environment, and Institute of Theoretical and Simulational Chemistry, the Academy of Fundamental and Interdisciplinary Science, Harbin Institute of Technology, Harbin, Heilongjian 150080, China

Supporting Information

ABSTRACT: We have studied single-walled carbon nanotubes (SWCNTs) doped with transition metal (TM) atoms with both exo and endo doping configurations. The electronic and geometric properties of these TM-doped SWCNTs were calculated within density functional theory. It was found that the endo-doped SWCNTs are less stable than the exo-doped counterparts due to the large geometric strain of the deformation in the endo-doped nanotubes. On the basis of partial charge analysis, the TM-doped SWCNTs have localized net charge distributions, whereas the spin densities in Sc-, Co-, and Cu-doped SWCNTs are delocalized over the entire nanotubes. The TM-doped SWCNTs are mostly metallic or narrow-gap semiconductive. With highly localized frontier molecular orbitals, the exo-doped SWCNTs are better electron donors than the corresponding endo-doped systems. As the dopant TM changes from Sc to Zn in the same row of the periodic table or from the top to the bottom in the same Pt group, the energy of the highest occupied crystal orbital of the TM-doped SWCNTs decreases, indicating a reduced electron donating ability.

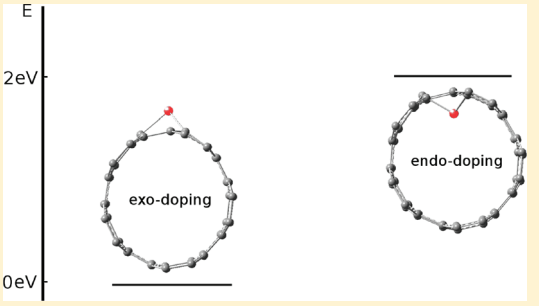

1. INTRODUCTION

Chemistry and physics of carbon allotropes, especially fullerene and carbon nanotubes (CNTs), have been one of the most active fields in the past two decades. Since the discovery of fullerene[1] and the first fabrication of multiwalled[2] and single-walled carbon nanotubes (SWCNTs),[3] substances containing carbon networks have been intensively and extensively studied with the goal of finding new materials. CNTs have such large longitudinal modules and low densities that they may be used as structural materials. Because the electronic structure of CNTs depends delicately on the nanotube parameters, such as tube diameter and chirality, selective use of individual CNTs or jointed CNTs (with different tube parameters) provides many opportunities for developing novel electronic devices.[4]

Functionalizations of fullerene and CNTs further expand the domain of application of these carbon-based materials. Many approaches have been designed and developed to functionalize CNTs, including doping light elements into defect sites[5] and ozonization at vacancy sites.[6] Among various functionalized CNTs, some are identified as potential new advanced materials. For instance, SWCNTs functionalized with specific polymers were found to be good candidates for ammonia detection.[7] Photoemission spectroscopic experiments and theoretical studies showed that atomic In transportation was influenced by the concentration of defects and offered a novel way to control the transportation of atoms.[8]

Ever since the first CNT came to the world, the fabrication of CNTs has been closely associated with numerous transition metal (TM) catalysts. Iron and its oxides are intimately involved in the growth mechanism of CNTs, in which the change of oxidation number of Fe plays an important role.[9] CNTs doped with different metal atoms, like Fe,[10] Sm,[11] and Pt,[12,13] were investigated for their potential catalytic and material utilities. Atomic chains of Cr and V adsorbed on CNTs are possible spintronic materials.[14] Some theoretical studies also indicated that SWCNTs coated with atomic Ti can become hydrogen storage materials.[15] Pt- and Ru-double-walled CNT adducts are efficient catalysts for direct methanol fuel cells.[16] Without a doubt, studies of interactions between TM atoms and CNTs not only provide effective ways to fabricate carbon-ring networks but also offer opportunities for discovering new materials or catalysts.

In the case of functionalized CNTs, the content and the position of the modification are crucial factors in determining the properties and reactivities of the resulting nanosystems. The wall of a fullerene or a single SWCNT divides the space into the interior and the exterior of the tubular system. Modifiers inside and outside nanotubes feel concave and convex surfaces, respectively, which possess very different chemistry and physics. This structural effect has been recently analyzed through the understanding of the bent conjugated π bonds in fullerenes and CNTs,[17] where the different curvatures of the two sides of a tubular wall lead to position-dependent properties and reactivities.

Received: October 2, 2009
Revised: March 25, 2011
Published: April 21, 2011

For example, an early theoretical study showed that the interior surface of a fullerene is inert to atomic hydrogen and atomic fluorine, whereas the exterior surface is highly reactive.[18] The novelty of the chemistry inside CNTs is particularly examplified by the Menshutkin S_N2 reaction, which was found to be much more favored within SWCNTs over the same reaction in the gaseous phase.[19] Experimental studies of the adsorption of various chemicals inside and outside SWCNTs have been critically reviewed, and attention has been drawn to the interaction between the oxidizers and the inner wall of SWCNTs.[20] The effect of confinement inside a SWCNT was also demonstrated in a chemical reaction between atomic hydrogen and heptene.[21] Aside from these few revealing studies of the chemical and physical properties of the inner wall of CNTs, the interior space has rarely been considered compared with the abundant results of the outer wall. It is necessary to further investigate the positional effect on the asymmetric curved tubular surface.

Thus far, the possibility of functionalizing curved carbon networks from the concave side has been studied mostly using theoretical tools. Studies of the functionalization of SWCNTs by carbene (CH_2), imine (NH), and atomic oxygen from both sides of the tubular wall showed that the lack of σ-bond formation from the concaved inner side of the SWCNT forces the light-element compounds to react preferentially with the outside of the nanotubes.[22] On the other hand, there have been some occurrences when heteroatoms stay on the inside concave surface. Using nuclear reaction techniques with the aid of theoretical calculations, the endohedral and substitutional Sb- and Te-doped fullerenes were made possible.[23] On the basis of density functional theoretical studies, the endo-Co-absorbed (8,8) SWCNT was found to be more stable than the exo absorbed one.[24] Different misalignments of carbon π orbitals from the interior or the exterior of SWCNTs may allow chemical species to stay preferentially inside the nanotubes. TM atoms, with their versatile bonding abilities and large radii, may have a better chance to reside steadily inside CNTs. We thus hope to find out whether some other heteroatoms, especially TM atoms, can be stably endo-doped into CNTs.

In what follows below, we report the results of our investigation into the possibility for a first-row TM atom to stay inside a (5,5) SWCNT after replacing a carbon atom of the tubular wall with the TM atom (Figure 1).

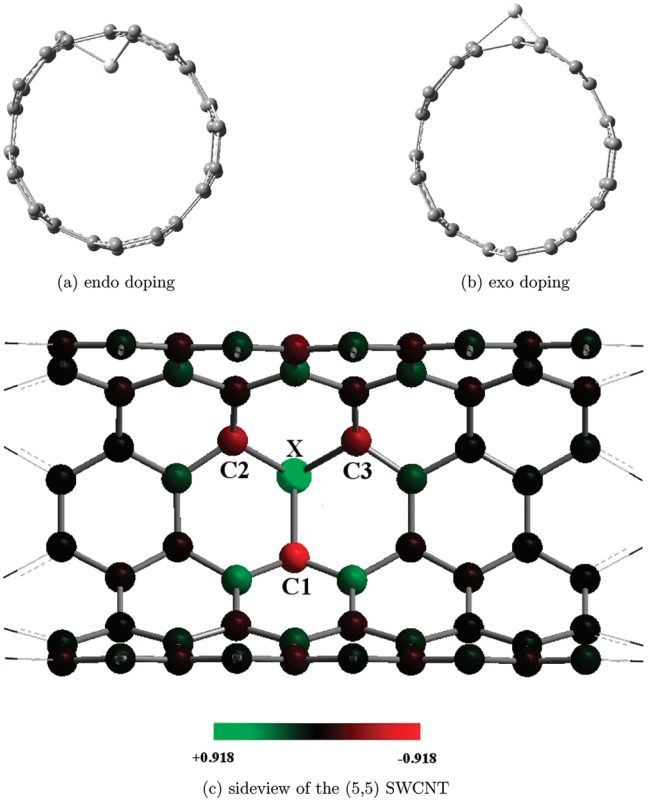

Figure 1. Schematic drawings of the model (5,5) SWCNT with partial charge distribution, doping site, and doping configurations. The dopant, labeled by "X", is surrounded by three neighboring carbon atoms (C1, C2, and C3). X−C1 is a vertical bond; X−C2 and X−C3 are slant bonds. The partial charge distribution in the exo-Sc-doped (5,5) SWCNT is also shown as a color overlay in (c). The values of partial charges are scaled according to the colored bar at the bottom. The color green indicates a positive charge and the color red, a negative charge. The darker the color (red or green), the larger the magnitude of the partial charge on the atom.

2. COMPUTATIONAL DETAILS

All calculations were performed using the Gaussian03 package.[25] The spin-unrestricted Kohn−Sham density functional method was adopted with the PBEPBE exchange-correlation functionals developed by Perdew, Burke, and Ernzohoff, which was improved in performance compared with PW91PW91 exchange-correlation functionals.[26] The electronic wave functions were expanded in the LanL2DZ atomic basis functions with the core shell electrons represented by the LanL2 pseudopotentials.[27] For consistence and comparison, LanL2DZ was applied to all elements.[13] Our current computational resources do not allow us to further increase the size of basis set beyond LANL2DZ for such systems. One-dimensional periodic boundary conditions were employed to model the (5,5) SWCNTs with 100 carbon atoms in the primitive cell (Figure 1c), with 40 k-points in the supercell. A carbon atom in the middle of the tube (labeled as "X" in Figure 1c) is replaced by a TM atom to model doped SWCNTs. Having realized the wall of the nanotube separates the space into the interior and the exterior, we placed the TM atom both inside and outside the tube hypersurface to investigate the positional effect. Since TM elements usually feature close-lying spin multiplicities, a large set of probable spin multiplicities for each doped SWCNT was fully considered for completeness. Geometry optimization was conducted without any symmetry constraint.

3. RESULTS AND DISCUSSIONS

In this study, the (5,5) SWCNT was chosen to be the prototype nanosystem for some specific reasons. If the selected nanotube has a very large diameter, the nanotube side wall will be extremely flat, resembling a single graphene sheet. The physics for the dopant being positioned inside or outside will be essentially the same; it is then meaningless to study. If the diameter is very small, the dopant atom inside the tube will come too close to those carbon atoms on the other end of the diameter opposite to the doping site. As a compromise, we have chosen the (5,5) SWCNT, which has a moderate tube diameter.

The relative stability of the TM-doped SWCNTs is compared in Table 1. For each TM element studied, the most stable structure is *always* the exo-doped. The lowest-lying endo-doped SWCNTs are less stable than the corresponding exo counterparts

Table 1. Relative Energies (in eV) for Each TM-Doped SWCNT of Different Doping Configuration and Spin Multiplicity[a]

dopant	configuration	relative energies (spin multiplicity, $\langle S^2 \rangle$)		
Sc	exo	0.000 (2, 0.7559)	0.916 (4, 3.7552)	2.547 (6, 8.7578)
	endo	2.361 (2, 0.7735)	2.815 (4, 3.7682)	4.096 (6, 8.7634)
Ti	exo	0.000 (1, 0.0000)	0.475 (3, 2.0056)	1.644 (5, 6.0054)
	endo	2.002 (1, 0.0000)	2.499 (3, 2.0035)	3.844 (5, 6.0059)
V	exo	0.000 (2, 0.8298)	0.382 (4, 3.7999)	1.494 (6, 8.7783)
	endo	2.138 (2, 0.8348)	2.791 (4, 3.8120)	3.997 (6, 8.7937)
Cr	exo	0.000 (3, 2.5668)	0.398 (5, 6.0870)	0.860 (1, 0.0000)
	endo	2.359 (3, 2.5758)	2.811 (5, 6.0878)	2.987 (1, 0.0000)
Mn	exo	0.000 (4, 3.8672)	0.030 (2, 1.2246)	0.603 (6, 8.8605)
	endo	2.069 (4, 3.8440)	2.230 (2, 1.5697)	2.770 (6, 8.8131)
Fe	exo	0.000 (1, 0.0000)	0.193 (3, 2.0458)	0.849 (5, 6.0743)
	endo	2.194 (1, 0.0000)	2.330 (3, 2.0784)	2.995 (5, 6.0330)
Co	exo	0.000 (2, 0.7687)	0.704 (4, 3.7750)	1.907 (6, 8.7720)
	endo	2.072 (2, 0.7726)	2.819 (4, 3.7744)	3.863 (6, 8.7737)
Ni	exo	0.000 (1, 0.0000)	0.052 (3, 2.0159)	0.884 (5, 6.0170)
	endo	1.886 (3, 2.0263)	2.038 (1, 0.0000)	2.732 (5, 6.0208)
Cu	exo	0.000 (2, 0.7647)		
	endo	2.562 (2, 0.8269)		
Zn	exo	0.000 (1, 0.0000)		
	endo	2.860 (1, 0.0000)		
Pd	exo	0.000 (1, 0.0000)	0.228 (3, 2.0118)	
	endo	2.783 (1, 0.0000)	2.908 (3, 2.0252)	
Pt	exo	0.000 (1, 0.0000)	0.289 (3, 2.0090)	
	endo	3.157 (1, 0.0000)	3.482 (3, 2.0157)	

[a] The data of the most stable exo- and endo-doped SWCNTs are shown in the third column. Spin multiplicities and calculated $\langle S^2 \rangle$ are shown as the first and second numbers in the parentheses, respectively.

by about 2.1 eV. This energy difference between the most stable endo- and exo-doped SWCNTs is relatively constant, irrespective of the type of the dopant TM. This implies that the stability variation mainly comes from the fluctuation in geometric strain from the exo to the endo doping configurations. This dominant effect of geometric strain is further supported by the observation that the energy difference between the endo- and exo-doped SWCNTs in any other same-spin state is very close to 1.9 eV, besides some extreme exceptions like the quartet Sc-doped SWCNTs. One may also find that some TM-doped SWCNTs are readily excited to another close-lying spin state: It costs no more than 0.1 eV to jump from the ground spin state to the nearest excited spin state for exo-Mn-, exo-Ni-, and endo-Fe-doped SWCNTs.

From the cross-section views shown in Figure 1, one can gather some common features shared by all TM-doped SWCNTs. The cross sections of the doped SWCNTs close to the doping site are oval and are different from the round cross section of the pristine SWCNT. C2 and C3 in the endo-doped SWCNTs point inward of the nanotube, while such atoms (C1, C2, and C3) in the exo-doped SWCNTs protrude out of the tube surface. Compared with the undeformed SWCNTs, the bonds pointing inward in the endo-doped SWCNTs create an even larger curvature, bending the six-membered carbon rings around the doping site away from the energetically favored, nearly planar aromatic structure. On the other hand, the extruding carbon atoms of the exo-doped SWCNTs alleviate much of the off-plane strain in the six-membered carbon rings containing C1, C2, and C3 carbon atoms. To verify this understanding, additional calculations were performed on the exo- and endo-Ti-doped SWCNTs. If we neglect the secondary change in the electronic structure after removing the Ti atom from the doped system, the energy difference between endo and exo dopings is about 0.9 eV, almost half of the energy difference between the endo- and exo-doped SWCNTs. The other remaining half of the total energy difference is primarily attributed to the lack of strong TM−carbon σ bonds in the endo-doped SWCNTs compared with the exo-doped SWCNTs.[22] In the endo-doped SWCNTs, the chemical bonds between the TM atoms and its three nearest carbon atoms are almost perpendicular to the other bonds of these carbon atoms. Normally, the carbon atoms of a SWCNT are sp^2 hybridized, in favor of coplanar σ bonds for the same carbon atom. In an endo-doped SWCNT, the TM atom bound to the carbon atoms from a perpendicular direction must experience some geometrical strain that also contributes to the instability of the doped nanotubes. Therefore, it is understandable that the exo-doped SWCNTs are energetically more stable than the endo-doped counterparts.

The endo-doped SWCNTs with first-row TM atoms are always substantially less stable than their exo counterparts, and their energy difference becomes even greater when the TM changes from Ni to Pt. For the second- and third-row TM atoms, the endo-doped SWCNTs are expected to be much more unstable than their exo counterparts because the energetic closeness of the valence s and d orbitals enhances the d character of the valence shell of later-row TM atoms.[28] This energy closeness makes the valence shell of late-row TMs exhibit more d character and thus leads to stricter orientational requirement of the bonds to the TM, which in turn exerts more strain in the endo-doped SWCNTs. Unlike the case of TM adsorption, in which the major bonding interaction between the TM atom and the CNT involves the p_π orbital of the carbon atoms, the adjustment of tubular structure can stabilize the TM absorbed inside certain SWCNTs, like Co in the (8,8) SWCNT.[24] In comparison, doping TM atoms into a single-vacancy defect site of a SWCNT internally, regardless of the geometric features of the SWCNT, will always be energetically unfavorable compared with external doping because of the large strain penalty in the endo doping.

From the optimized geometric parameters shown in Figure 2, we can gain more appreciation of structural features of the most stable exo- and endo-doped SWCNTs. Even without symmetry constraint during geometry optimization, most of the optimized structures, except for the endo-V-doped SWCNT, have essentially C_s symmetry with the mirror plane passing through the TM atom and perpendicular to the longitudinal direction. In the endo-V-doped SWCNT, the V atom is close to one of the slantwise-bonded carbon atoms, in favor of a lower energy from symmetry breaking. The bond lengths of TM atoms to the three closest carbon atoms in the doped SWCNTs are displayed in Figure 2. Whether the nanotube is endo- or exo-doped, the vertical X−C1 bond is longer than the two slant X−C2 and X−C3 bonds, except in the endo-Co-, endo-Fe-, and endo-Cu-doped SWCNTs. The longer X−C2 (X−C3) bond length indicates that the slant TM−carbon bond is weaker than the vertical TM−carbon bond. The TM−carbon bond lengths in the exo-doped SWCNTs are always larger than the corresponding bond lengths in the endo-doped systems. In comparison with the corresponding slant and vertical C−C bonds in the pristine (5,5) SWCNT, the TM−carbon bond is much longer: over 1.7 Å

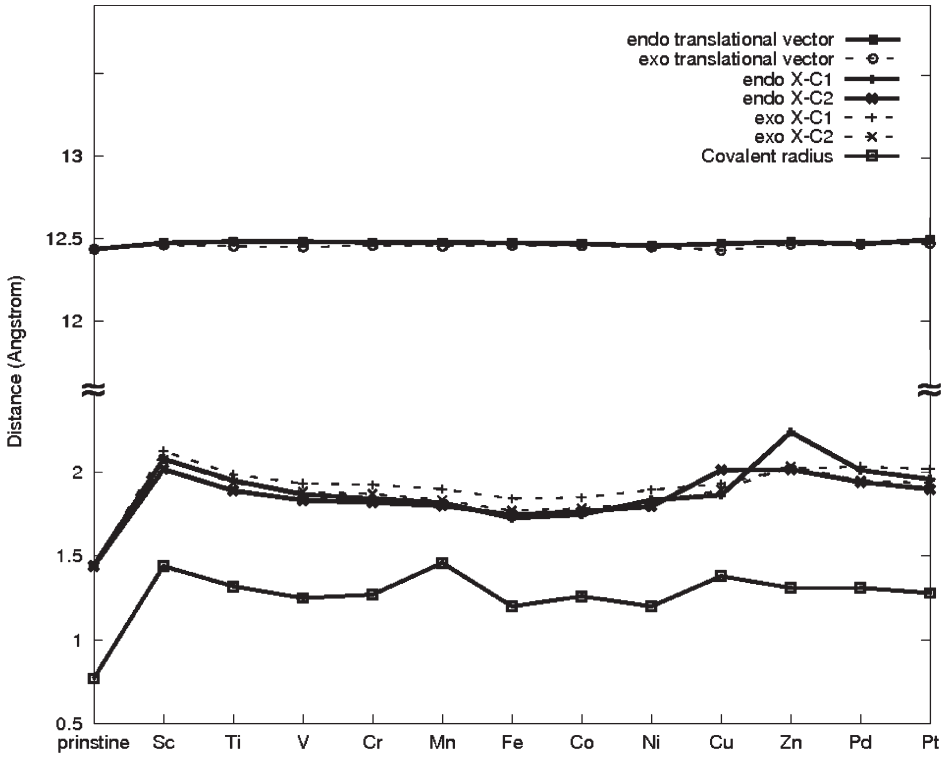

Figure 2. Geometric parameters of the pristine and TM-doped SWCNTs. The covalent radius of each element is reproduced from ref 29. Translational vectors are indicators of the elongation along the longitudinal direction.

(vs 1.4 Å). However, the extended bonds around the doping site do not evoke significant tubular elongation because the heteroatom is positioned far away from the tubular surface, which reduces the amount of elongation along the longitudinal direction.

Following the Periodic Table from the left to the right in the first row of TM, the atomic size gets smaller except for Cr and Cu whose ground-state electronic configurations change from the preceding $4s^2 3d^n$ to $4s^1 3d^{n+1}$. However, TM−carbon bond lengths do not follow this trend in the doped SWCNTs: the TM−carbon bond length decreases from Sc to Fe and increases from Co to the last element Zn in this row. Particularly, Cu- and Zn-doped SWCNTs exhibit very long TM−carbon bonds. For Ni-, Pd-, and Pt-doped SWCNTs, the Pd−C bond is longer than the Pt−C bond, and both bonds are still longer than the Ni−C bond because of lanthanide contraction. The V-, Cr-, and Mn-doped SWCNTs have similar TM−carbon bond lengths because these TM-doped SWCNTs have a gradual increment in the spin multiplicity and therefore have the same number of valence electrons to form chemical bonds.

The spin multiplicities, spin densities, and atomic partial charges on the metal atoms are collected in Table 2. It is well-known that elements become less metallic from the left to the right in the same row of the Periodic Table. So, along the same direction, the calculated partial charge on the TM atom decreases, and the TM−carbon bond gradually evolves from being highly ionic to being somewhat covalent. Also in the same direction, the TM atom of an endo-doped SWCNT carries less (positive) charge than does the same TM atom of the exo-doped systems. Most partial charges are located within the first four layers of carbon atoms around the TM atom. This is well illustrated in the exo-Sc-doped SWCNT (Figure 1c), which has the largest partial charge on the TM dopant atom in this study. For the open-shell species, SWCNTs doped with Sc and Co are spin polarized by the TM atoms, whereas SWCNTs doped with V, Cr, and Mn are characterized by localized spin densities on the TM atoms.

Table 2. Calculated Partial Charges and Spin Densities of the Most Stable Endo- and Exo-Doped SWCNTs[a]

dopant	multiplicities	spin densities	partial charges
Sc	2, 2	−0.009, 0.038	0.703, 0.918
Ti	1, 1		0.512, 0.748
V	2, 2	0.838, 1.241	0.420, 0.626
Cr	3, 3	2.496, 2.638	0.416, 0.553
Mn	4, 4	2.648, 2.715	0.365, 0.547
Fe	1, 1		0.063, 0.216
Co	2, 2	0.194, 0.267	0.022, 0.299
Ni	3, 1	0.396	−0.057, 0.430
Cu	2, 2	0.089, 0.055	−0.006, 0.553
Zn	1, 1		0.626, 0.825
Pd	1, 1		−0.190, 0.334
Pt	1, 1		0.362, 0.892

[a] In columns 2−4, the first and second numbers of each pair are for the endo- and exo-doped systems, respectively.

The frontier molecular orbitals are important in interpreting chemical reactivity. We thus exhibit the highest occupied crystal orbitals (HOCOs) and lowest unoccupied crystal orbitals (LUCOs) in Figure 3. Most of the doped SWCNTs are narrow-gap semiconductive or (semi)metallic with their Fermi levels around −4.0 eV. Most of the frontier orbitals of the TM-doped SWCNTs are localized near the doping site, either directly

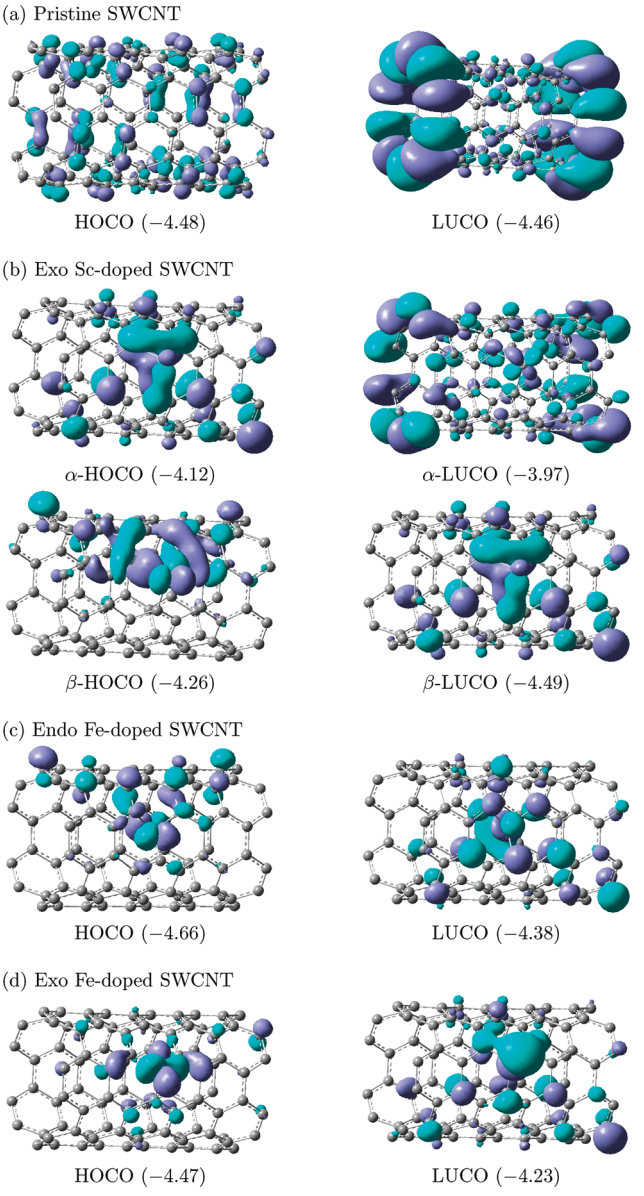

Figure 3. Frontier crystal orbitals of the pristine, Sc-, and Fe-doped SWCNTs. Orbital energies (in eV) are shown in parentheses.

on the dopant TM atom or on the closest surrounding carbon atoms. The HOCO energies of the endo-doped SWCNTs are usually lower than those of the exo counterparts by several tenths of an electronvolt, indicating a slightly reduced electron donating ability. When the TM changes from Sc to Zn (except for Mn, Co, and Zn), the HOCO energy, along with the electron donating ability, decreases from −4.2 to −4.5 eV. When the dopant TM atoms are from the same Pt group, the doped SWCNTs show comparable trends in the electronic properties.

The exo-Sc-doped SWCNT, unlike most other TM-doped SWCNTs, opens an α-spin gap while being β-spin conductive (see Figure 4). This trait in the electronic structure makes the exo-Sc-doped SWCNT potentially a spin polarizer that can transport electricity with a single spin state.[14] In both exo- and endo-Sc-doped SWCNTs, α-spin HOCOs are quite different from α-spin LUCOs, but β-spin HOCOs are very similar to β-spin LUCOs in both spatial distributions and orbital energy

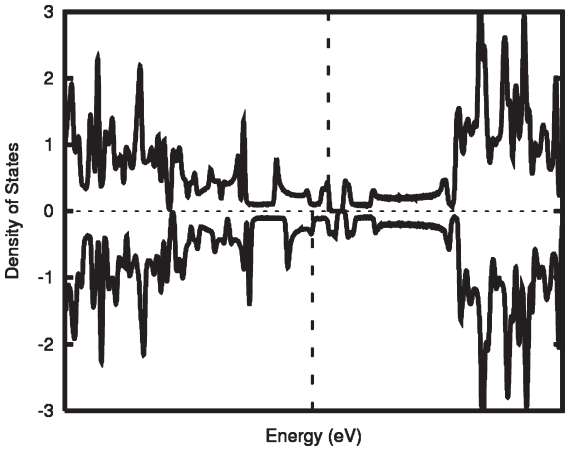

Figure 4. Density of states (DOS) of the exo-Sc-doped (5,5) SWCNT. The DOS of α-spin and β-spin electrons are shown in the upper and lower panels, respectively. Fermi levels are marked by the vertical dotted lines.

(nearly degenerate). The same understanding can be applied to explain the small band gaps of the endo-V-doped SWCNT (in α spin) and in the Fe- and Ni-doped SWCNTs. The HOCO and the LUCO of the Sc-doped SWCNTs mainly consist of the neighboring carbon p_π orbitals surrounding the Sc atom. In both endo- and exo-Ti-doped SWCNTs, the HOCOs are mostly composed of carbon p orbitals, while the LUCOs are made of p orbitals of the carbon atoms and the 3d orbitals of the Ti atom. If the TM is V, more 3d orbitals of V are involved in forming the frontier orbitals. The endo-Cr-doped SWCNT has a HOCO largely made from the Cr atom, the major electron donation center in the system. The Mn-doped SWCNTs, though with higher spin multiplicities instead, have their frontier orbitals concentrated on the carbon atoms where the reactive site lies. Regardless of the doping configurations, the Fe-doped SWCNTs feature large Fe contribution to both the HOCO and the LUCO. In the Co- and Ni-doped SWCNTs, the frontier orbitals are mainly built from surrounding carbon p orbitals. The exo-Ni-, exo-Pd-, and exo-Pt-doped SWCNTs have very similar band structures to the pristine SWCNTs near the Fermi level (see Figure 1S in the Supporting Information). On the other hand, the endo-Ni-, endo-Pd-, and endo-Pt-doped SWCNTs have more localized HOCOs with lower orbital energies.

4. CONCLUSION

We have studied the exo- and endo-TM-doped (5,5) SWCNTs in an effort to find the stable TM-doped SWCNTs and to investigate their properties. The introduction of TM atoms does not significantly elongate the nanotube along the longitudinal direction. The endo-TM-doped SWCNTs are found to be less stable than their exo counterparts by about 2 eV due to the unfavorable TM−carbon bonding interaction and the deformation of the host nanotube upon endo doping. The net charge distribution in a TM-doped SWCNT is mostly localized within the first four layers of the carbon atoms surrounding the dopant TM atom. The spin density of open-shell systems, on the other hand, can be quite delocalized in such systems as the Sc-, Co-, and Cu-doped SWCNTs. The electron-donating ability of the exo-TM-doped SWCNTs are superior to their corresponding endo systems. As the TM changes from the

left to the right in the first *d*-block of the Periodic Table, the HOCO energy decreases and the doped SWCNT becomes less reactive toward electrophiles. When the SWCNT is doped with TM atoms from the Pt group, though with similar electronic structures, the endo-doped SWCNTs are much less stable than the exo ones. We further argued that the SWCNTs endo-doped with second- and third-row TM atoms are much more unstable than their exo counterparts, simply because of the collapsing space among the valence s and d orbitals in the second- and third-row TM elements, which will induce more structural strain due to stronger directional bonding with increased d character in the frontier molecular orbitals.

■ ASSOCIATED CONTENT

Supporting Information. Band structures and geometries of endo- and exo-doped SWCNTs. This material is available free of charge via the Internet at http://pubs.acs.org.

■ AUTHOR INFORMATION

Corresponding Author
*E-mail: yawang@chem.ubc.ca.

■ ACKNOWLEDGMENT

Financial support for this project was provided by a grant from the Natural Sciences and Engineer Research Council (NSERC) of Canada. W.Q.T. is grateful for the support from the State Key Lab of Urban Water Resource and Environment at HIT (grant No. 2009TS01).

■ REFERENCES

(1) Kroto, H. W.; Heath, J. R.; O'Brien, S. C.; Curl, R. F.; Smalley, R. E. *Nature* **1985**, *318*, 162–163.
(2) Iijima, S. *Nature* **1991**, *354*, 56–59.
(3) Iijima, S.; Ichihashi, T. *Nature* **1993**, *363*, 603–605.
(4) Avouris, P. *Acc. Chem. Res.* **2002**, *35*, 1026–1034.
(5) Liu, L. V.; Tian, W. Q.; Wang, Y. A. *J. Phys. Chem. B* **2006**, *110*, 1999–2005.
(6) Liu, L. V.; Tian, W. Q.; Wang, Y. A. *J. Phys. Chem. B* **2006**, *110*, 13037–13044.
(7) Bekyarova, E.; Kalinina, I.; Itkis, M. E.; Beer, L.; Cabrera, N.; Haddon, R. C. *J. Am. Chem. Soc.* **2007**, *129*, 10700–10706.
(8) Barinov, A.; Üstünel, H.; Fabris, S.; Gregoratti, L.; Aballe, L.; Dudin, P.; Baroni, S.; Kiskinova, M. *Phys. Rev. Lett.* **2007**, *99*, 046803.
(9) Smalley, R. E.; Li, Y.; Moore, V. C.; Price, B. K.; R., C., Jr.; Schmidt, H. K.; Hauge, R. H.; Barron, A. R.; Tour, J. M. *J. Am. Chem. Soc.* **2006**, *128*, 15824–15829.
(10) Billas, I. M. L.; Massobrio, C.; Boero, M.; Parrinello, M.; Branz, W.; Tast, F.; Malinowski, N.; Heinebrodt, M.; Martin, T. P. *Comput. Mater. Chem.* **2000**, *17*, 191–195.
(11) Lu, G.; Deng, K.; Wu, H.; Yang, J.; Wang, X. *J. Chem. Phys.* **2006**, *124*, 054305–054309.
(12) Tian, W. Q.; Liu, L. V.; Wang, Y. A. *Phys. Chem. Chem. Phys.* **2006**, *8*, 3528–3539.
(13) Yeung, C. S.; Liu, L. V.; Wang, Y. A. *J. Phys. Chem. C* **2008**, *112*, 7401–7411.
(14) Yang, C. K.; Zhao, J.; Lu, J. P. *Nano Lett.* **2004**, *4*, 561–563.
(15) Yildrim, T.; Ciraci, S. *Phys. Rev. Lett.* **2005**, *94*, 175501.
(16) Li, W.; Chen, X. W. Z.; Waje, M.; Yan, Y. *J. Phys. Chem. B* **2006**, *110*, 15353–15358.
(17) Lu, X.; Chen, Z. *Chem. Rev.* **2005**, *105*, 3643–3696.
(18) Mauser, H.; Hirsch, A.; van Eikema Hommes, N. J. R.; Clark, T. *J. Mol. Model.* **1997**, *3*, 415–422.
(19) Halls, M. D.; Schlegel, H. B. *J. Phys. Chem. B* **2002**, *106*, 1921–1925.
(20) Kondratyuk, P.; J. T. Yates, J. *Acc. Chem. Res.* **2007**, *40*, 995–1004.
(21) Kondratyuk, P.; J. T. Yates, J. *J. Am. Chem. Soc.* **2007**, *129*, 8736–8739.
(22) Zheng, G.; Wang, Z.; Irle, S.; Morokuma, K. *J. Am. Chem. Soc.* **2006**, *128*, 15117–15126.
(23) Ohtsuki, T.; Ohno, K.; Shiga, K.; Kawazoe, Y.; Maruyama, Y.; Shikano, K.; Masumoto, K. *Phys. Rev. B* **2001**, *64*, 125402–125406.
(24) Yagi, Y.; Briere, T. M.; Sluiter, M. H. F.; Kumar, V.; Farajian, A. A.; Kawazoe, Y. *Phys. Rev. B* **2004**, *69*, 075414.
(25) Frisch, M. J.; Trucks, G. W.; Schlegel, H. B.; Scuseria, G. E.; Robb, M. A.; Cheeseman, J. R.; Montgomery, J. A.; Vreven, T.; Kudin, K. N.; Burant, J. C.; Millam, J. M.; Iyengar, S. S.; Tomasi, J.; Barone, V.; Mennucci, B.; Cossi, M.; Scalmani, G.; Rega, N.; Petersson, G. A.; Nakatsuji, H.; Hada, M.; Ehara, M.; Toyota, K.; Fukuda, R.; Hasegawa, J.; Ishida, M.; Nakajima, T.; Honda, Y.; Kitao, O. ; Nakai, H.; Klene, M.; Li, X.; Knox, J. E.; Hratchian, H. P.; Cross, J. B.; Bakken, V.; Adamo, C.; Jaramillo, J.; Gomperts, R.; Stratmann, R. E.; Yazyev, O.; Austin, A. J.; Cammi, R.; Pomelli, C.; Ochterski, J. W.; Ayala, P. Y.; Morokuma, K.; Voth, G. A.; Salvador, P.; Dannenberg, J. J.; Zakrzewski, V. G.; Dapprich, S.; Daniels, A. D.; Strain, M. C.; Farkas, O.; Malick, D. K.; Rabuck, A. D.; Raghavachari, K.; Foresman, J. B.; Ortiz, J. V.; Cui, Q.; Baboul, A. G.; Clifford, S.; Cioslowski, J.; Stefanov, B. B.; Liu, G.; Liashenko, A.; Piskorz, P.; Komaromi, I.; Martin, R. L.; Fox, D. J.; Keith, T.; Al-Laham, M. A.; Peng, C. Y.; Nanayakkara, A.; Challacombe, M.; Gill, P. M. W.; Johnson, B.; Chen, W.; Wong, M. W.; Gonzalez, C.; Pople, J. A. *Gaussian 03*; Gaussian, Inc.: Wallingford, CT, 2004.
(26) Perdew, J. P.; Burke, K.; Ernzerhof, M. *Phys. Rev. Lett.* **1996**, *77*, 3865–3868.
(27) Hay, P. J.; Wadt, W. R. *J. Chem. Phys.* **1999**, *82*, 299.
(28) Frenking, G.; Fröhlich, N. *Chem. Rev.* **2000**, *100*, 717.
(29) Porterfield, W. W. *Inorganic Chemistry: A Unified Approach*, 2nd ed.; Academic: New York, 1993.